Reservoir Static Modelling towards Safe CO₂ Storage in Depleted Oil Reservoirs of 'CRK' Field, Niger Delta, Nigeria

U. U. Mkpese ᵃ*, G. O. Emujakporue ᵃ and A. O. Sofolabo ᵃ

ᵃ Department of Physics, University of Port Harcourt, Choba, Rivers State, Nigeria.

Authors' contributions

This work was carried out in collaboration among all authors. All authors read and approved the final manuscript.

Original Research Article

ABSTRACT

Geological carbon storage (GCS) is gradually gaining acceptance as the technology of highest repute for the mitigation against greenhouse gas effect. This involves the injection and long-term or permanent storage of carbon dioxide (CO_2) in subsurface geological formations. The development of a robust 3D reservoir model then becomes necessary to understand the facies changes and the petrophysical properties distribution of candidate CO_2 storage reservoirs. This study attempts the use of static modelling technique to investigate the depleted oil and gas reservoirs of 'CRK' field in the Niger Delta sedimentary Basin as a potential CO_2 storage site. Using an integrated approach of 3D seismic and a suit of well logs from the study area, two reservoir sands (D10C0 and D6200) were mapped. 3D static modelling of discrete and continuous property distribution of the reservoirs revealed the reservoirs are composed majorly of clean sands with water saturation ranging from 8 to 75%. The average porosity and permeability values are between 20 to 29% and 250 to 890mD respectively. A theoretical storage capacity of 24.85Mt is estimated for the two reservoirs combined, while the median effective storage capacity is 6.22Mt. Comparison of the results obtained in the

_____

*Corresponding author: E-mail: mkpese.uu@gmail.com;

study with recommended standard values show the reservoirs are suitable for CO_2 storage. The property models constructed can serve as primary input for dynamic simulation of the oilfield in future studies.

Keywords: CO_2 storage; greenhouse gas; static modelling; storage capacity; petrophysical properties.

1. INTRODUCTION

Carbon dioxide (CO_2) has attracted worldwide attention for its role in the depletion of ozone layer causing global warming and the consequent potential threats it poses to human existence. The global greenhouse gas emissions from energy-related sources takes up over 73% of total emissions of which gas flaring is considered a significant contributor, while those from agriculture, industry waste and land use take the remaining 27% [1]. An average of about 150×10^9 cubic meters of associated gas from crude production have been reportedly flared globally each year going back to mid-1990s up till recent as revealed by data from various advanced satellite monitoring tools, along with voluntary reporting [2].

Oil production has remained the major source of carbon emission in Nigeria. Currently, it is the only African country rated among the top seven gas flaring countries in the world running for nine years now, with Russia leading the group [3]. It is reported that about 40% of produced gas is flared, re-injecting only about 12% to enhance oil recovery in the Niger Delta region [4]. According to a projection by the International Energy Agency (IEA), global energy demand is likely to increase well close to 4% by year 2030 with fossil fuels remaining the major source [5]. In contributing to net-zero campaign [6], it is necessary to adopt mitigation technologies which are capable of reducing the amounts of these anthropogenic gases released into the atmosphere, especially those from crude production in the Niger Delta region

Geological carbon capture and storage (CCS) which involves the capturing, transporting and storing of CO_2 in subsurface geological formations has been regarded as a technology of the highest potential for reducing CO_2 emissions from the combustion of fossil fuels in the short-to-long term [5]. Such geological formations include the deep saline aquifers, depleted oil/gas reservoirs and unminable coal beds amongst others which all contribute to an amazing global theoretical storage capacity of between 8, 000 and 55, 000Gt [6]. While storage in deep saline aquifers is regarded as having the largest theoretical capacity [6], it is however, hindered by some uncertainties and challenges such as significant variation of storage capacity, limited information on geological characteristics, high costs associated with infrastructure construction, and the risk of CO_2 and brine leakage [7]. Hence, depleted oil and gas reservoirs becomes the next most preferred option for geologic CO_2 sequestration owing to a number of reasons: (i) These reservoirs have been extensively studied for their geological structures and physical properties; (ii) It is assumed that since these reservoirs have originally accumulated hydrocarbon, notably a higher carbon content chemical in traps, for millions of geological years then they are also capable of holding CO_2 for either re-use of permanent storage; (iii) There are vast array of computer models already developed in the oil and gas industry to predict the movement, displacement behaviour, and trapping of fluids in these reservoirs; (iv) Existing infrastructures and wells already in place may be used for handling CO_2 storage operations which will eventually reduce costs; and finally (v) storage in depleted hydrocarbon reservoirs can be optimized to enhance oil/gas recovery [8,9].

Generally, as a potential CO_2 sink, the subsurface formation must present with certain desirable characteristics such as having a good seal rock to prevent vertical flow to the ground surface, a large storage volume to store significant quantities of CO_2, be deep enough (at least 800 m) to keep CO_2 at supercritical state [7,9], be leak-free and be reasonably permeable to allow for the injection of CO_2 at reasonable rates from a reasonable number of wells [9]. Details of the processes involved in capturing and storing CO_2 in subsurface geological formations have been extensively discussed in [10,11,12].

In order to access a good fit for resource estimation, optimize production efficiency, enhance cost-effectiveness and economic feasibility of subsurface resources, the technique of 3D modelling of rock properties and fluid characteristics has been adopted and used for decades [13,14,15]. This involves incorporating

seismic data, core samples, well logs and other geological information to create a comprehensive representation of rock properties in three-dimensional space [16]. In its very adequacy, 3D modelling allows for revealing the distribution of reservoir properties even in multiplex reservoirs with lateral and vertical lithologic variations, leading to enhanced volumetric estimation, risk and uncertainty analysis, predictions of fluid flow and field development plans. This technique is also proving useful as an integral aspect of appraisal studies targeted at any potential CO_2 storage site for its injectivity, capacity and retention assessment by building a robust 3D static model of the geologic formations of interest [14,15].

Although there has been several 3D static modelling attempt at some reservoir units of the Niger Delta basin, notably the works of Adeoti et al. [13], Hammed et al. [17] and Kura et al. [16], all of which were targeted mainly at hydrocarbon prospectivity and reserves estimation without commenting on the implications for carbon sequestration. Also, recent studies on carbon capture and storage in the region have focused primarily on general review of the technology [5,7], capacity estimations [18,19] and assessment of the structural and stratigraphic competence of some reservoir units of the basin [20,21]. However, none of those works looked at the 3D reservoir properties assessment as it favours CO_2 storage in the region, except for Yahaya-Shiru et al. [21] while investigating the reservoir units of the Central Swamp Depositional Belt which is relatively of closer proximity to the population than the Coastal Swamp Depositional Belt where the present study is situated, especially considering the risk of leak-off. In this work, we attempt the integration of 3D seismic data, well logs and other available geological information for the production of robust 3D static property models of an oilfield of the Niger Delta to ascertain its suitability as a potential CO_2 sink. The property models which will also serve as the primary inputs for dynamic simulation of the oilfield in future study will include discrete reservoir properties such as the facies distribution and the continuous spatial distribution of petrophysical properties such as total porosity, permeability and water saturation.

1.1 Location and Geological Background

The study area is an oilfield within the Coastal Swamp Depositional Belt of the onshore Niger Delta which has been code-named 'CRK' field. Fig. 1 describes the approximate location of the study area; its actual name and further details about its location were withheld due to certain confidentiality agreement. The Niger Delta, situated in the Gulf of Guinea along the West Africa Margin, lies between longitude 5 °E to 8 °E and latitude 4 °N to 6 °N [16]. It is deemed one of the most prolific deltaic provinces in the world in terms of hydrocarbon accumulation and has a clastic wedge sedimentary thickness of up to 12km [22]. The formation of the delta involved a balance between subsidence and sedimentation rates during which the tectonic setting and structural configuration of the region played a crucial role in influencing the depositional pattern of the sediment [23]. There are three distinct formations identified within the Niger Delta sedimentary basin; the marine Akata, paralic Agbada, and continental Benin Formations. The Akata Formation serves as the primary source rock and consists mainly of marine shale while the Agbada Formation comprises of sandstone with intercalations of shale, making it the key reservoir rock. The Benin Formation, on the other hand, consists of coarse grained, gravelly, poorly sorted, sub-angular to well-rounded sands. It is the most prolific aquifer in the region and comprises over 90% massive, porous sands with localized clay/shale inter-beds [22,23].

2. MATERIALS AND METHODS

2.1 Dataset

The dataset used in this study was provided by Shell Petroleum Development Company (SPDC) with permission from the Nigerian Upstream Petroleum Regulatory Commission (NUPRC) formerly the Department of Petroleum Resources (DPR). The dataset includes 3D seismic volume (SEG-Y format), wireline logs, formation tops, checkshot data and biostrat data. The wireline logs had mainly Gamma Ray, Neutron Density, Resistivity and Spontaneous Potential logs. Data for four wells were provide, namely: *CRK-01, CRK-025, CRK-029 and CRK-032*, all within the seismic cube (Fig. 1).

2.2 Lithology and Reservoir Identification

Gamma ray and resistivity logs are useful tools in determining lithology and reservoir zones respectively. Shale-free sandstones and carbonates have low concentrations of radioactive material and give low gamma ray readings and high or low values of resistivity

depending on the fluid content. In this study, lithology identification was done using the gamma ray log, usually calibrated with a scale range of 0 to 150 American Petroleum Institute (API) units, by setting the shale base line to a constant value of 65 API [25]. This shale base line served as a consistent reference across the entire CRK field for identifying shale formations. Any values in the range ≤ 65 API represents a sandstone formation. Delineation of pay zones (i.e hydrocarbon bearing zones) was done by using a combination of both the gamma ray and resistivity logs aided by the provided formation tops. A relatively high resistivity response which correlates with a sand formation is interpreted as a hydrocarbon bearing zone.

2.3 Seismic Analysis

Seismic interpretation is carried out to ascertain the structural framework of the studied field. In doing this, fault structures and other initial trapping mechanisms in the study area are revealed. Usually, the first step in seismic interpretation is to conduct a seismic-to-well tie to establish the exact position of the reservoir sands on the seismic section as well as the lateral extent and geometry of the reservoirs [14,15]. In performing a well-to-seismic tie, two key log data: density and sonic as well as check shot data are required to generate the reflection coefficients (RC) and acoustic impedance (AI) based on the principle of convolution [25]. The
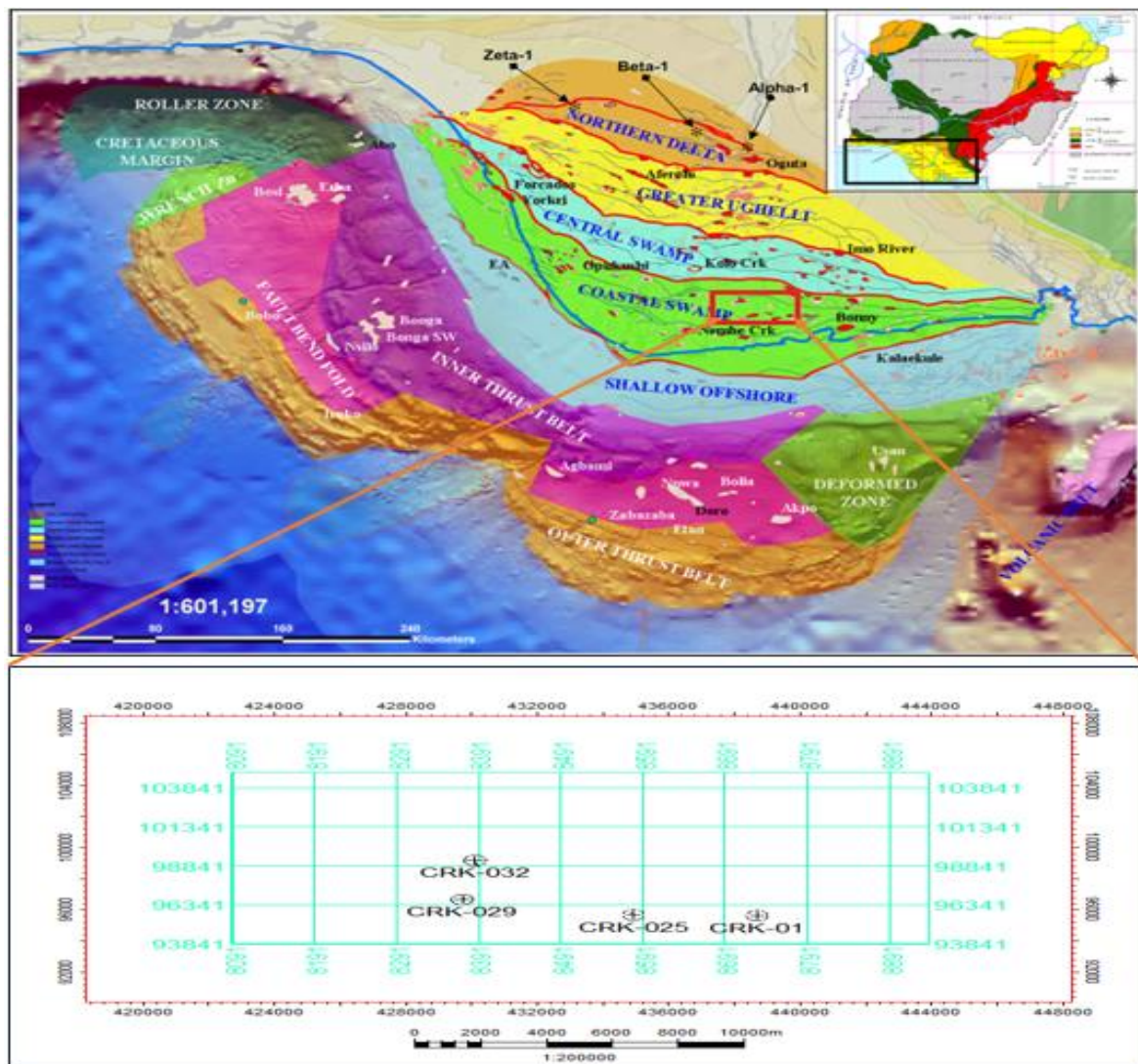

Fig. 1. Map of the Niger Delta showing approximate location of CRK field, with wells and seismic cube of the field produced from Schlumberger Petrel (Modified after [24])

well tie in this study was done using the check shot data from well *CRK-01* because it had density and sonic log data which were normally distributed and appeared more robust than the other wells. A befitting synthetic seismogram was generated using a Ricker wavelet of 25Hz which was then used to tie the wells to seismic. This was followed by mapping structural discontinuities (faults) over the entire seismic volume and picking of seismic horizons corresponding to reservoir tops on the well logs [15,25]. The faults in the seismic section contained within the reservoir zones are extracted and digitized [14]. And, finally, the mapped horizons were used to generate reservoir surfaces in time and thereafter converted to depth maps [15,25] using the Schlumberger Petrel 2021.2 software.

2.4 Petrophysical Evaluation

Both the qualitative and quantitative petrophysical evaluation of the field was done using the Techlog software by Schlumberger Limited. A combination of the wireline logs such as the gamma ray, sonic, density and resistivity logs were used for the lithology discrimination and in estimating the reservoir properties. Petrophysical properties such as porosity (ϕ), Permeability (K), water saturation (S_w), Volume of Shale (V_{SH}), Net-to-Gross (N/G), reservoir thicknesses and caprock thicknesses were estimated from the available wireline logs following the methodology and standard formulae documented in [13,16,18].

For instance, the total porosity (ϕ) was estimated using Tixier formula with density log being the key input [16,18];

$$\phi = \frac{\rho_{ma} - \rho_b}{\rho_{ma} - \rho_f} \qquad (1)$$

Where ρ_b is bulk density (i.e the input density log), ρ_{ma} is density of rock matrix and ρ_f is fluid density given the values 2.67g/cm^3 and 0.8 g/cm^3 respectively [16]. The reservoir effective porosity was then obtained by applying shale correction [26];

$$\phi_{eff} = \phi \, (1 - V_{SH}) \qquad (2)$$

The fluid saturation of a reservoir is the fluid volume expressed as a function of the total pore space; the fraction pore space containing water is termed water saturation (S_w). Although it is one of the most challenging petrophysical parameters

to calculate, but it is useful for estimating hydrocarbon saturation (1-S_w). In this work, water saturation (S_w) was calculated using the Udegbunam's relation [16];

$$S_w = \frac{0.082}{\phi}; \qquad (3)$$

Where ϕ is the porosity calculated from log data.

Permeability (K) was determined using the Owolabi empirical relation [13,16] which is believed to be more suitable for the Niger Delta sands as it accounts for the unconsolidated reservoir sand of the hydrocarbon province [16]. The expression is given as;

$$K = 307 + 26552(\phi^2) - 34540(\phi \times S_w)^2 \qquad (4)$$

Where ϕ is the formation porosity and S_w is water saturation.

2.5 Reservoir Static Modelling

3D static models were built for the reservoirs by integrating relevant geological data and the interpretations discussed in preceding sections. The modelling process starts with building the reservoir structural model which envelopes a larger framework of the reservoir. Key input elements include the faults and boundary surfaces which are then populated with varying petrophysical properties. Fault sticks are converted to fault polygons and utilized as input in a fault modelling process to generate a faulted 3D grid. A skeletal grid comprising of the faults and key pillars is constructed in a process called "Pillar Gridding" resulting in skeletal structural model as shown in Fig. 2. Another process involves the insertion of the horizons into the faulted 3D grid where the grid is then associated with time or depth maps and/or well tops as inputs. Having done this, a final step was to make a fine scale layering ready and suitable for facies and property modelling. The statistical analysis tool embedded in the Petrel software, sequential indicator simulation (SIS), was generally used in modelling the facies distribution while the sequential Gaussian simulation (SGS) algorithm was used for the distribution of continuous properties allowing the assigned property values in the log from the penetrated wells to be distributed both vertically and horizontally to fill the whole 3D grid [15]. In general, a spherical variogram type was used for all properties with an anisotropy range set to 1978.1 and 9451.63 at major and minor directions respectively. To quality check and

validate the models created, a bulk volume and cell inside-out geometric properties were generated which showed no negative values and no distorted cells for the both properties respectively as shown in Fig. 3.

2.6 Static Capacity Estimates

The estimation of CO_2 static capacity is a straightforward process; most approaches use various analytic formulae [10,14,18,27] derivable from either the volumetric and/or compressibility estimation of the reservoir resources to deduce storage capacity. In the case of volumetric approach, the key input parameter is the reservoir pore volume or the initial stock

tack oil/gas in place. In this study, the estimation of static CO_2 storage capacity was done following the Carbon Sequestration Leadership Forum (CSLF) scheme for oil and gas reservoirs [27], which is based on the assumptions that the volume previously occupied by the produced hydrocarbons becomes available for CO_2 storage, and that CO_2 will be injected into depleted oil and gas reservoirs until the reservoir pressure is brought back to the original reservoir pressure. For oil reservoirs, the effective storage capacity in each reservoir is calculated on the basis of its recoverable oil reserves, its reservoir properties and in situ CO_2 characteristics based on the following expression [27];
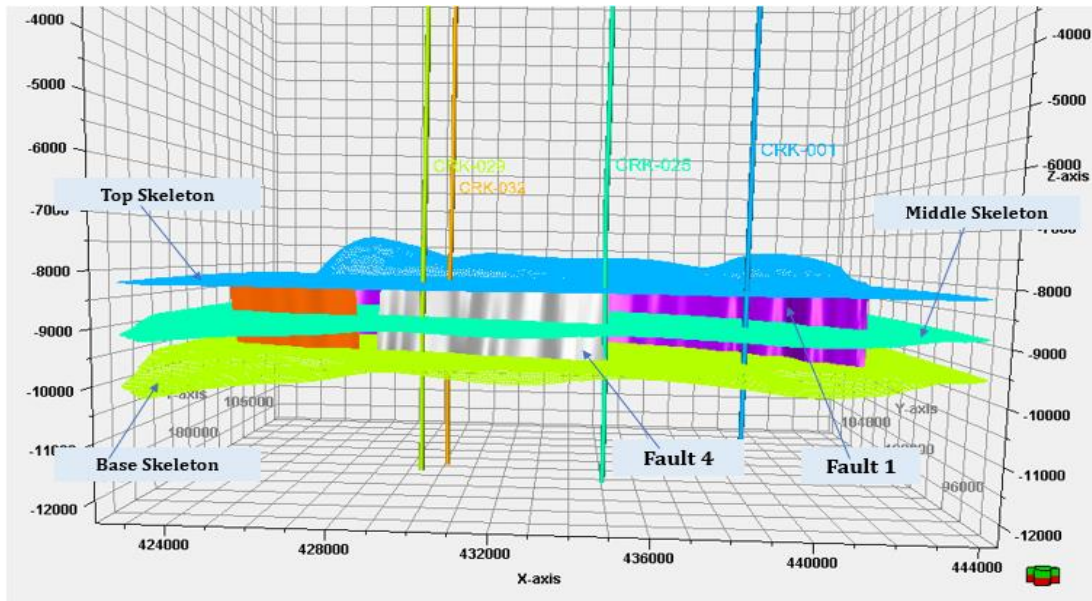

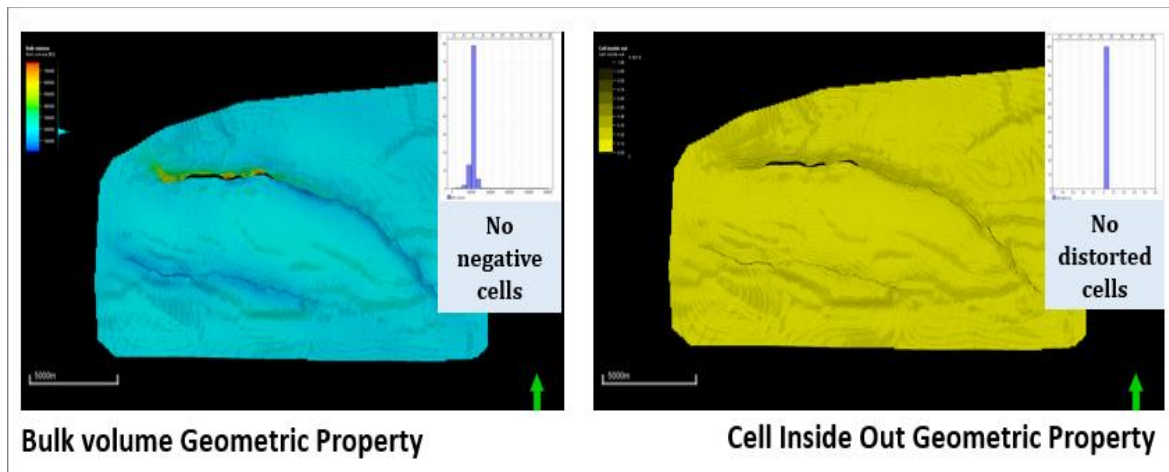**Fig. 2. 3D grid components for Reservoir D10C0**

Fig. 3. 3D Static modelling quality check

369

$$M_{CO2e} = \rho_{CO2} \times R_f \times STOIIP \times B_o \times C_e \qquad (5)$$

Where M_{CO2e} is the effective storage capacity (Mt), $STOIIP$ is the stock tank oil initially in place (Stb), ρ_{CO2} = density of CO_2 (Kg/m³), B_o is oil reservoir volume factor, R_f is recovery factor and C_e is the effective capacity coefficient factor $(0 < C_e < 1)$ [27].

The storage coefficient C_e for oil/gas fields is equivalent to the *E* factor for saline formations in terms of defining a portion of the theoretical storage capacity as the effective storage capacity [30].

3. RESULTS AND DISCUSSION

Analysis of the provided well logs and formation tops revealed there were potentially several reservoir units in the studied field. However, the requisite logs were sparsely distributed across the wells and, as such, interpretations were made using a combination of the logs and the formation tops as a blind guide. Two reservoir units D10C0 and D6200 with their corresponding seal pairs were confidently delineated with traceable lateral continuity across a minimum of three wells. The mapped reservoirs (D10C0 and D6200) are within the Agbada formation which is considered the most prolific formation for explorable hydrocarbons in the region and buried deep enough to support the sequestration of supercritical CO_2. A combination of the gamma-ray logs together with neutron density and resistivity logs were useful in identifying reservoir fluid contents and contacts. The resistivity logs, particularly, exhibit significant high signatures within the identified reservoir units which depicts hydrocarbon-bearing zones. Further scrutiny with the neutron density logs also revealed the reservoirs are oil sands. Fig. 4 depicts the positions of the reservoirs and their corresponding seal pairs after seismic-to-well tie. Also, a summary of the average reservoir properties including reservoir and caprock thicknesses generated from analyses of the well logs are presented in Table 1.

Table 1. Average reservoir properties from log analysis

Res. Zone	Res. thickness (m)	ϕ (%)	K (mD)	NTG	S_w (%)	Cap. thickness (m)
D10C0	15.97	26	560.81	0.87	32	29.10
D6200	39.81	21	282.45	0.52	26	109.12

Res. Zone = Reservoir Zone, Res. thickness = Reservoir Thickness, Cap. thickness = Caprock Thickness, Φ = Porosity, K =Permeability and Sw =water saturation
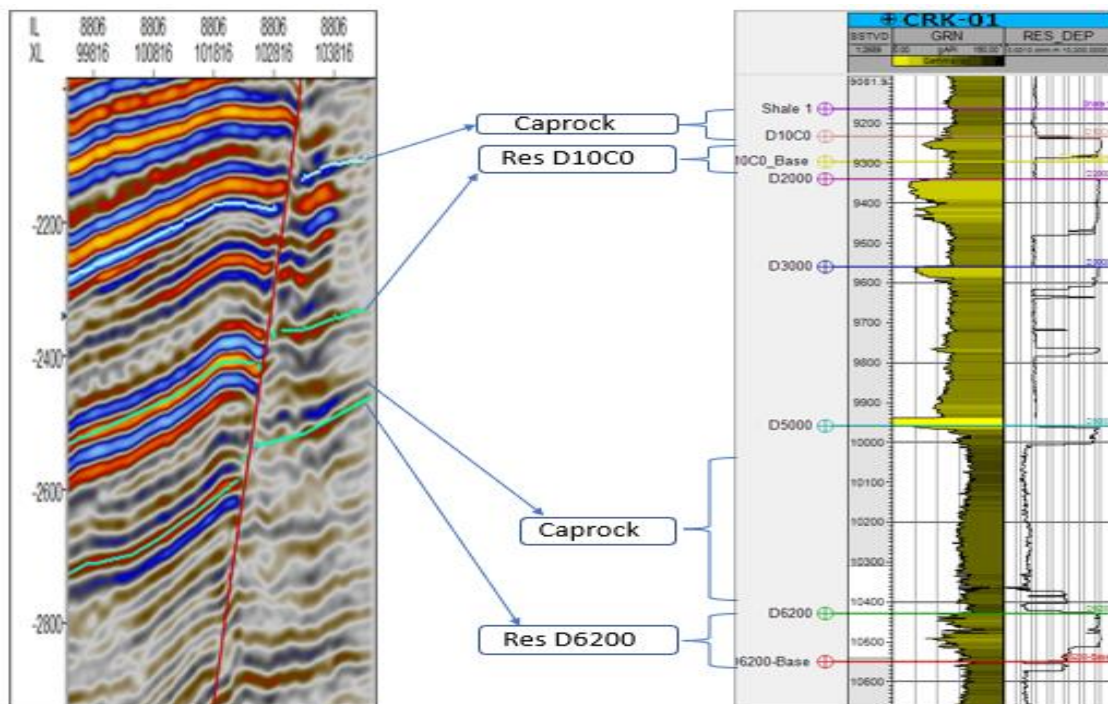

Fig. 4. Reservoir-seal pairs of CRK field

The structural interpretations of the seismic section reveal the presence of regional, synthetic and antithetic faults in the area. The mapped faults and horizons are shown in Fig. 5. Fault 1 (*F1*) is a regional fault which was seen extending almost the entire breadth of the mapped area while the rest of the faults are minor faults forming a network of both synthetic and antithetic faults. The interplay of all faults divided the field into upthrown and downthrown blocks with observable fault closures and associated rollover anticlinal structures and collapse crests which are potential hydrocarbon traps [22]. The time contour maps of the horizons of interest showed marked increase in two-way travel times from the northern to the southern area, with maximum values reaching 2.4s indicative of low structural features in the northern parts and high structure features in the southern parts [15]. Also, the generated depth maps revealed a pattern of anticlinal closures (rollover anticlines) within the faults network. Such closures possess efficient traps suitable for hydrocarbon accumulation and potentially good traps for CO_2 storage in the field.

3D static modelling of the reservoir properties revealed the reservoirs are mostly clean sands. Four facies, Shale, Sandy Shale, Shaly Sand and Sand, were modelled following the typical sand-shale depositional environment of the Niger Delta sedimentary Basin. Analysis of the facies distribution trend indicates that both sand and shale occur in all the modelled zones with predominantly sand bodies. In reservoir D6200, the sand composition (Shaly Sand and Sand) is about 68.2%, while in reservoir D10C0 it is about 62.9%. Fig. 6 (a-d) and Fig. 7 (a-d) shows the property distribution models for reservoir D10C0 and D6200 respectively, with different colour coding describing portions of the models with low and high values of the different reservoir properties. The reservoir property models revealed porosity distribution prominently around 0.2 to 0.29 and permeability values dominant within the range of 250 to 890mD for the two reservoirs. These values of porosity and permeability are indicative of the pore space having the ability to easily accept and accumulate sufficient fluid increasing the reservoirs' storage capacity. Water saturation models revealed typically low values of the property for the both reservoirs with values ranging from between 8% to about 75%, predominant values are generally below 17% and corresponds to reservoir areas with high porosity indicating high hydrocarbon saturation.
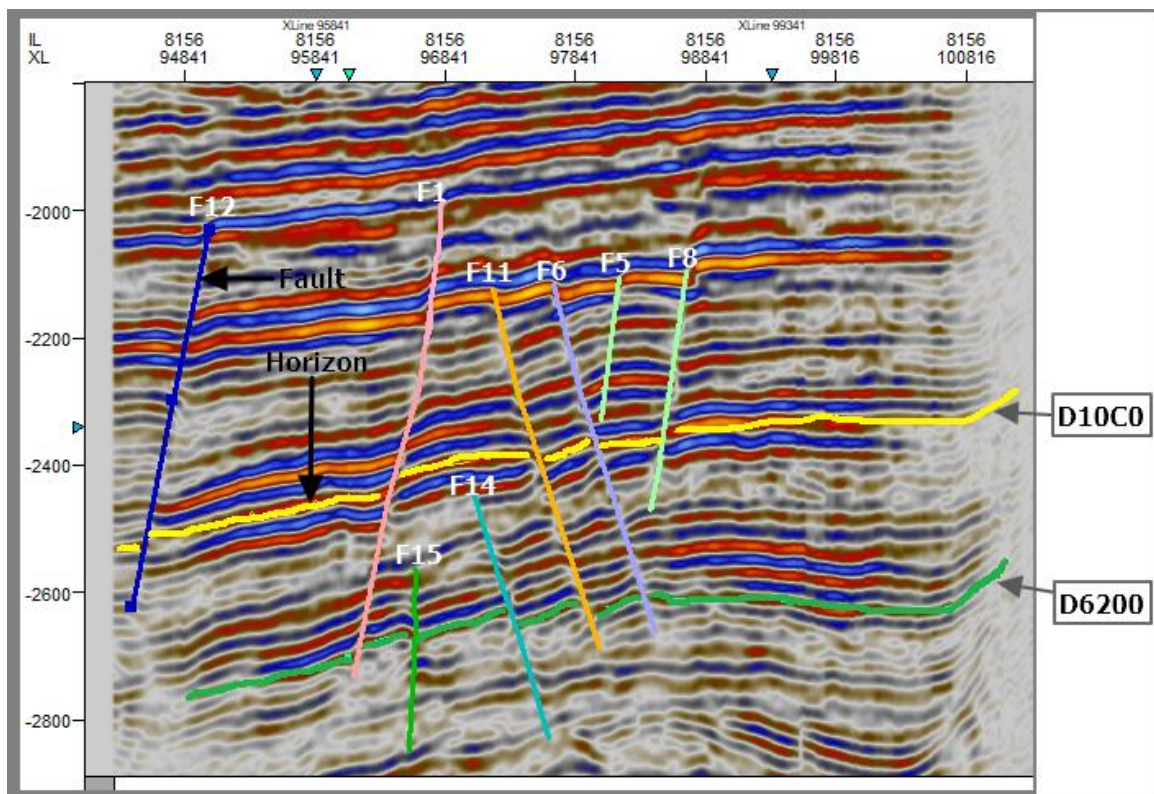

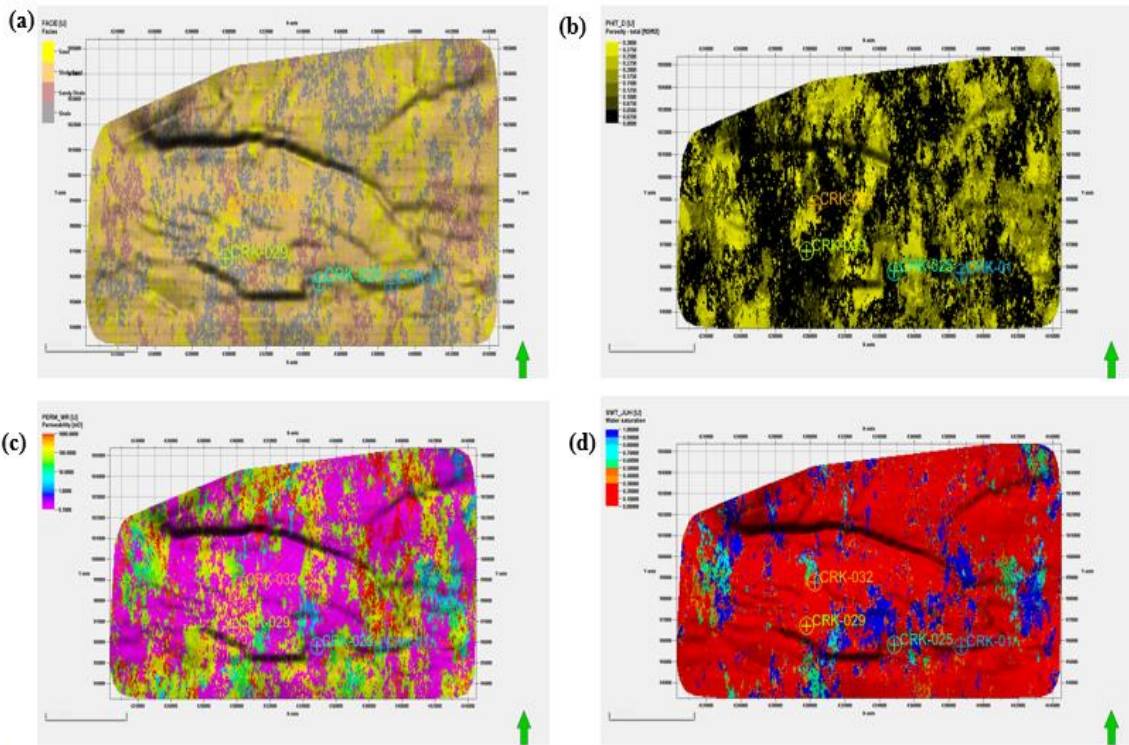**Fig. 5. Some interpreted Faults and Horizons on Seismic Inline 8156**

Fig. 6. Modeled property distribution of reservoir D10C0 (a) Facies, (b) Porosity (c) Permeability and (d) Water Saturation
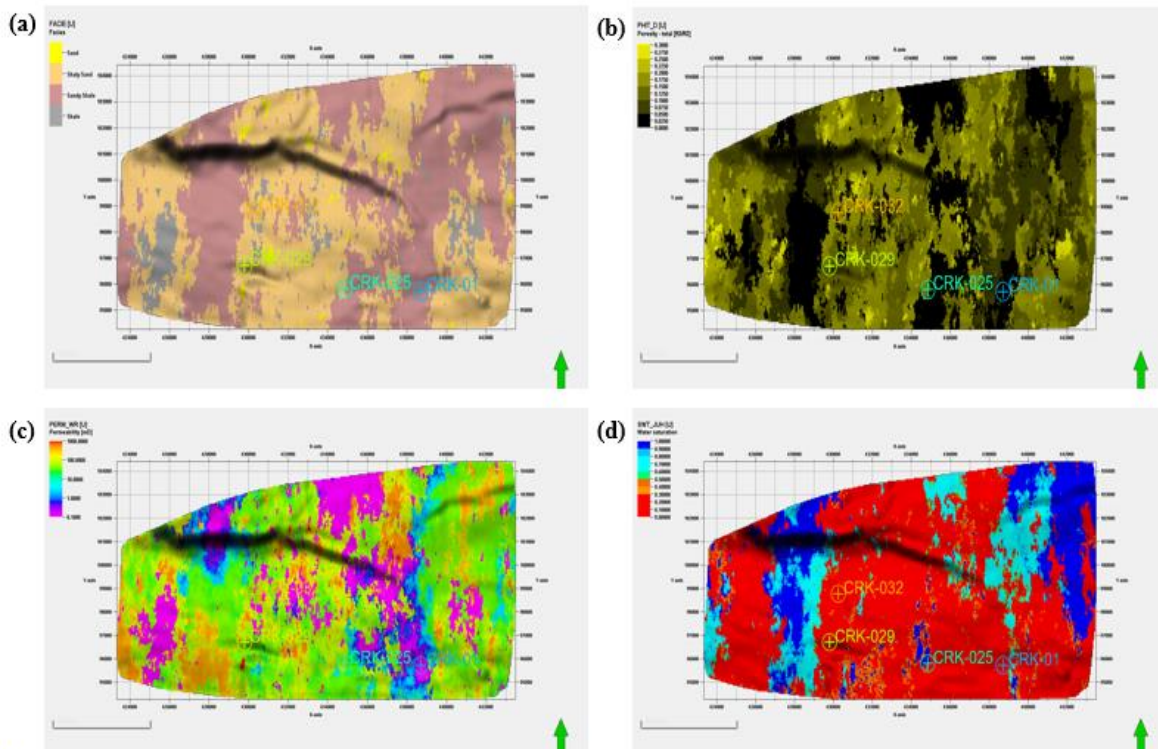

Fig. 7. Modeled property distribution of reservoir D6200 (a) Facies, (b) Porosity (c) Permeability and (d) Water Saturation

Noticeably, while water saturation is porosity controlled, it is observed that the distribution of petrophysical properties in the reservoirs are generally controlled by the facies distribution. For instance, reservoir D6200 exhibits high to medium porosity and permeability values with increasing prominence in the western, central and southeastern portions of the reservoir which corresponds to areas of the reservoir with predominantly Sand and Shaly Sand facies.

According to the classification presented in Table 2 [28], the evaluated reservoirs of 'CRK' field can be considered good reservoirs based on their 'very good' porosity and permeability values. Also, as shown in Table 3, the results obtained in this work compares favourably with recommended minimum values extracted based on the screening criteria of IEA [11] and Ramírez [29] which shows the reservoirs are qualified as potential CO_2 sinks.

Volumetrics of the reservoirs after modelling as well as the computed static CO_2 storage capacity of CRK field were also obtained. Reservoir D10C0 is estimated to have a bulk volume of 0.513×10^6 acre-ft which corresponds to stock tank oil in place (STOIIP) and recoverable oil volumes of 239.70×10^6 STB and 107.86×10^6 STB based on a 45% recoverable factor while reservoir D6200 has a bulk volume, STOIIP and recoverable oil volumes of 1.3×10^6 acre-ft, 171.06×10^6 STB and 76.97×10^6 STB respectively. Reservoir D10C0 appears to be more prolific and offers an increased pore space that can accommodate sequestered CO_2

Table 2. Qualitative ranking of rock porosity and permeability [28]

ϕ (%)	Qualification	K (mD)	Qualification
0 – 5, 5 - 10	Negligible, Poor	<10.5	Poor to Fair
10-15	Fair	15 - 50	Moderate
15 – 20	Good	50 - 250	Good
20 – 25	Very good	250 - 1000	Very Good
>30	Excellent	>1000	Excellent

Φ = Porosity and K =Permeability.

Table 3. Computed reservoir and caprock properties of CRK Field

Parameter	Minimum Threshold [11,29]	This Study
Reservoir composition	Limestone, sandstone, siltstone, carbonates (For hydrocarbon fields)	Sandstone
Depth to top	≥800 m	2816m to 3289m
Reservoir thickness	≥10 m	16m to 40m
Reservoir porosity	> 10%	15% to 29%
Reservoir permeability	>200mD	250 to 890mD
Seal thickness	Salt, anhydrite, shale or claystones	Shale
Seal thickness	≥10 m. (applies to both simple and complex seals)	29m to 109m
Storage capacity	4 Mt for gas/oil reservoirs	24.85Mt

Table 4. Reservoir Volumes and Computed CO_2 Storage Capacity of CRK Field

Parameters		Res D10C0	Res D6200	Both
CO_2 Density (t/m^3)		0.65	0.65	
Volume Factor (bbl/stb)		1.3	1.3	
Recovery Factor (%)		45	45	
Bulk Volume (10^6 acre-ft)		0.513	1.301	1.814
STOIIP (10^6 stb)		239.70	171.06	410.76
REC Oil (10^6 stb)		107.86	76.97	184.83
Theoretical CO_2 Storage, M_{CO2} (Mt)		14.50	10.35	24.85
Effective CO_2 Storage, M_{CO2e} (Mt)	C_e=0.12	1.74	1.24	2.98
	C_e=0.25	3.63	2.59	6.22
	C_e=0.40	5.80	4.14	9.94

Res = Reservoir, STOIIP = Stock tank oil initially in place, REC Oil = Recoverable oil, CO2 = Carbon dioxide, t/m3 = Metric tons per cubic metre, bbl = Barrels, stb = Stock tank barrels, Mt = Millions metric tons

probably because of its higher net-to-gross and low water saturation values compared to that of reservoir D6200. A summary of these estimates and parameters used are presented in Table 4.

The candidate reservoirs under consideration are within the depth range of 2500–3500m which is much within the recommended depth range that is sufficient to keep CO_2 at supercritical state [27]. Under supercritical conditions, CO_2 has a liquid-like density of approximately 500-800 kg/m^3 [30], so that the volume of the CO_2 is significantly reduced compared to the gas phase at shallower depths. Considering the mild-to-average geothermal gradient of the region reported as 13.46 to 33.66 ^oC /km [18], it is reasonable to estimate the storage capacity using an average CO_2 density of 650 kg/m^3 (0.65Mton/m^3). The C_e factor of values 0.12, 0.25 and 0.4 were used for capacity reduction based on the work of Zhou et al. [31]. These values correspond to a low-end, mid and high-end values indicative of the worst case to best case scenarios.

The estimated total theoretical storage of CO_2 in the oilfield is 24.85Mt while the effective storage capacities range between 2.98 to 9.94Mt. The total theoretical storage of the field compared to the recommended 4Mt minimum storage shows the oilfield qualifies as a potential CO_2 sink. However, this result is likely an underestimation since only two reservoirs in the field were considered due to lack of data; if all the reservoirs were to be accounted for, the storage capacity would far exceed this number.

4. CONCLUSION

The aim of this work was to conduct 3D static reservoir modelling of 'CRK' field of the Niger Delta basin to ascertain its suitability for injection and storage of CO_2 which is now believed to be a more potent means to reduce CO_2 emission into the atmosphere. The Niger Delta is generally known for releasing large amounts of these anthropogenic gases through gas flaring from the production of crude oil.

3D static property modelling has been conducted for the reservoir units of the study area using the integrated approach of 3D seismic and well log data. The resulting models reveal the discrete distribution of reservoir facies and continuous rock properties distribution within the field are within the desirable characteristics for a potential CO_2 storage site. Two reservoirs with traceable lateral continuity were identified from the petrophysical analysis of the four wells and the provided formation tops. The distribution of porosity and permeability in the reservoirs which are prominently around 0.2 to 0.29 and 250 to 890mD respectively allows for the classification of the reservoirs as good reservoirs, and hence, suitable for CO_2 injection and storage.

The depleted oilfield promises a bulk pore volume which corresponds to a theoretical storage capacity of 24.85Mt and a median effective storage capacity estimate of 6.22Mt. Arguably, the values presented in this work could be considered an underestimation owing to lack of data; the storage capacities would far exit these values assuming all reservoir units in the field were accounted for, however, the estimates are based on data made available. Moreover, these values already surpass the minimum selection criteria for a potential CO_2 storage site in terms of sequestrable mass of CO_2. This study presents an adequate investigation into the CRK oilfield and establishes its suitability as a potential CO_2 storage site. The models can now serve as the primary input for dynamic simulation modelling of CO_2 storage in the field.

ACKNOWLEDGEMENTS

COMPETING INTERESTS

Authors have declared that no competing interests exist.

REFERENCES

1   Ritchie H, Roser M, Rosado P. CO_2 and greenhouse gas emissions. Our World in Data; 2023.
     Available:https://ourworldindata.org/ co2-and-greenhouse-gas-emissions
     Accessed on: 29 March, 2023.
2   Anonymous. Global gas flaring and oil production (1996-2018). World Bank; 2019.

Available:https://pubdocs.worldbank.org/en/18210156018537968/pdf/Global-gas-flaring-and-oil-production-1996-2018.pdf
Accessed on: 21 March 2023.

3 Anonymous. Global gas flaring tracker report. World Bank; 2023.
Available:https://www.worldbank.org/en/programs/gasflaring reduction/publication/global-gas-flaring-tracker-report
Accessed on:12 September, 2022.

4 Onyekonwu M. Best practices and policies- the Nigerian Oil and Gas industry policy problems. Port Harcourt Petroleum Review. 2008;1(1):14.

5 Yelebe ZR, Samuel RJ. Benefits and Challenges of implementing carbon capture and sequestration technology in Nigeria. Engineering. 2015;42–49.

6 Raimund M, Samantha M. The world has vast capacity to store CO2: Net zero means we'll need it. IEA Commentary. 2023;01:04.
Available:https://www.iea.org/commentaries/the-world-has-vast-capacity-to-store-co2-net-zero-means-we-ll-need-it
Accessed on:2 July, 2023

7 Akpanika OI, Etim JO, Udoh FD. Diverting CO_2 emissions from the atmosphere through capture and geologic sequestration: The Journey So Far! J Environ Earth Sci. 2015;5(2):42-52.

8 Benson SM, Cook P. In: Freund, P. (Ed.), Underground geological storage, in intergovernmental panel on climate change special report on carbon dioxide capture and storage. Cambridge Univ. Press, Cambridge, U.K. 2005;195–276.

9 Agartan E, Gaddipati M, Yip Y, Savage B, Ozgen C. CO2 storage in depleted oil and gas fields in the Gulf of Mexico. Int J Greenh Gas Control. 2018;72:38–48.

10 Shaw J, Bachu S. Screening, evaluation, and ranking of oil reservoirs suitable for CO2-Flood EOR and carbon dioxide sequestration. JCPT. 2002;41(9).

11 IEA. CO2 storage in depleted gas fields: Global application criteria for carbon dioxide enhanced oil recovery. IEA-GHG technical study report no. 2009;12.

12 Godec M, Koperna G, Petrusak R, Oudinot A. Assessment of factors influencing CO2 storage capacity and injectivity in Eastern U.S. Gas Shales. Energy Procedia. 2013; 37:6644-6655.

13 Adeoti L, Onyekachi N, Olatinsu O, Fatoba J, Bello M. Static reservoir modeling using well log and 3-d seismic data in a KN field, Offshore Niger Delta, Nigeria. Int J Geosci. 2014;5:93-106.

14 Afolayan BA, Mackay E, Opuwari M. 3D Static modeling and CO2 static storage estimation of the hydrocarbon-depleted charis reservoir, Bredasdorp Basin, South Africa. Nat Resour Res; 2023.
Available:https://doi.org/10.1007/s11053-023-10180-w

15 Ali AM, Radwan AE, Abd El-Gawad EA, Abdel-Latief AS. 3D integrated structural, facies and petrophysical static modeling approach for complex sandstone reservoirs: A case study from the coniacian-santonian matulla formation, July Oilfield, Gulf of Suez. Egypt. Nat Resour Res. 2021;31(1):385–413.

16 Kurah BK, Shariatipour MS, Itiowe K. Reservoir characterization and volumetric estimation of reservoir fuids using simulation and analytical methods: A case study of the coastal swamp depobelt, Niger Delta Basin, Nigeria. J Pet Exp Product Technol. 2021;11:2347–2365.
Available:https://doi.org/10.1007/s13202-021-01206-1

17 Hammed O, Koledoye B, Ajao K, Ojero J, Jackson C, Sunday O, Adekun A. Integrated 3D reservoir modeling for the delineation of sand body geometry and heterogeneity: Implication for hydrocarbon potential assessment of "GMEDAL" field, Offshore, Niger Delta. NAPE Bulletin. 2020;29(1):89-107.

18 Ojo AC, Tse AC. Geological characterisation of depleted oil and gas reservoirs for carbon sequestration potentials in a field in the Niger Delta, Nigeria. J Appl Sci Environ Mgt. 2016;20(1):45-55.

19 Ubani CE, Ikpaisong US, Uti OS. Sequestration of CO2 in depleted reservoirs: A case study of a Niger Delta Field. Int. Res. J Adv Eng Sci. 2019;4(1):264-269.

20 Umar BA, Gholami R, Nayak P, Shah AA, Adamu H. Regional and field assessments of potentials for geological storage of CO2: A case study of the Niger Delta Basin, Nigeria. J Nat Gas Sci Eng. 2020; 77;1-17.

21 Yahaya Shiru M, Igwe O, Obafemi S. 3D structural and stratigraphic characterization of X feld Niger Delta: Implications for CO2 sequestration. J Pet Exp Product Technol. 2021;12:959–977.

22   Doust H, Omatsola E. Niger Delta. In: Edwards JD, Santogrossi PA (eds) Divergent/passive margin basins. Am Asso Pet Geol. Bulletin Memoir, Tulsa, 1990; 48:239–248.

23   Kulke H. Regional petroleum geology of the world. Part II: Africa, Australia and Antarctica. Berlin, Gebruder Bogrntraeger. 1995;143–172.

24   Oluwajana OA, Ehinola OA, Okeugo CG, Adegoke O. Modeling hydrocarbon generation potentials of eocene source rocks in the agbada formation, Northern Delta Depobelt, Niger Delta Basin, Nigeria. J Pet Exp Product Technol. 2017;7:379–388.

25   Fagbemigun TS, Ayuk MA, Oyanameh OE, Akinrinade OJ, Amosun JO, Sanuade AO, et al. Hydrocarbon reservoir characterization of "Otan Ile" feld, Niger Delta. J Pet Exp Product Technol. 2021; 11:601–615.

26   Al-Ruwaili. Accuracy of shaly sand formation evaluation. United States Patent. 2007; Patent no. US 7,168, 310 B2.

27   Bachu S, Bonijoly D, Bradshaw J, Burruss R, Holloway S, Christensen NP, et al. CO_2 storage capacity estimation: Methodology and gaps. Int. J. Greenh. Gas Control. 2007;1:430–443.

28   Etu-Efeotor, JO. Fundamental of petroleum geology. Paragraphics, Port Harcourt; 1997.

29   Ramírez A, Hagedoorn S, Kramers L, Wildenborg T, Hendriks C. Screening CO_2 storage options in The Netherlands. Int. J. Greenh. Gas Control. 2010;4(2):367-380.

30   DOE–NETL. Best practices: Site screening, site selection, and site characterization for geologic storage projects. Revised Edition; 2017.

31   Zhou D, Zhao Z, Lie P, Liao J, Zhang Y, Zhang C. et al. Assessment of CO_2 storage potential for guangdong province, China. Global CCS Institute. South China Sea Institute of Oceanology; 2013.

Peer-review history:
The peer review history for this paper can be accessed here:
https://www.sdiarticle5.com/review-history/114325